JPET Fast Forward. Published on July 27, 2007 as DOI: 10.1124/jpet.107.126680

JPET #126680

A novel oral indoline-sulfonamide agent, J30, exhibits potent activity against human cancer cells *in vitro* and *in vivo* through the disruption of microtubule

Jing-Ping Liou, Kuo-Shun Hsu, Ching-Chuan Kuo, Chi-Yen Chang, Jang-Yang Chang

College of Pharmacy, Taipei Medical University (J.-P.L.); National Institute of Cancer Research, National Health Research Institutes (K.-S.H., C.-C.K, C.-Y.C., J.-Y.C.); Division of Hematology/Oncology, Department of Internal Medicine, Tri-service General Hospital, National Defense Medical Center (J.-Y.C.), Taipei, Taiwan, Republic of China

Running title: A novel oral indoline-sulfonamide agent targets tubulin

Correspondence to: Dr. Jang-Yang Chang, National Institute of Cancer Research, National Health Research Institutes, 7th Floor, No.161, Section 6, Ming-Chuan East Road, Taipei 114, Taiwan, R.O.C., Tel: 886-2-2653-4401 ext. 25110, Fax: 886-2-2792-9654, E-mail: jychang@nhri.org.tw

Number of Text Pages: 26

Number of Tables: 2

Number of Figures: 6

Number of References: 32

Number of Words in Abstract: 194

Number of Words in Introduction: 596

Number of Words in Discussion: 794

Abbreviations:

CPT, camptothecin; ECL, enhanced chemiluminescence; FBS, fetal bovine serum; HRP, horseradish peroxidase; J30, N-[1-(4-Methoxy-benzenesulfonyl)-2,3-dihydro-1H-indol-7-yl]-Isonicotinamide; *Ki*, inhibition constant; MDR/Pgp, multidrug resistance P-glycoprotein; MRP, multidrug-resistance associated protein; NOD/scid mice, non-obese diabetic/severe combined immune-deficiency mice; PARP, poly(ADP-ribose) polymerase; PBST, phosphate buffered saline with 0.1% Tween-20; PI, propidium iodide; PVDF, polyvinylidene difluoride; SDS-PAGE, sodium dodecyl sulphate-polyacrylamide gel electrophoresis; Taxol, paclitaxel; VP16, etoposide

Abstract

We have previously synthesized a series of 7-Aroyl-Aminoindoline-1-Sulfonamides as a novel class of antitubulin agents. Here we show that one of these new compounds, J30, is potently effective against various resistant and non-resistant cancer cell lines despite the status of MDR, MRP, or other resistance factors *in vitro*. J30 inhibits assembly of purified tubulin by strongly binding to the colchicine-binding site. Western blot and immunofluorescence experiments demonstrate that J30 depolymerizes microtubules in the KB cell line, resulting in an accumulation of G2/M phase cells. Further studies indicate that J30 causes cell cycle arrest, as assessed by flow analyses and the appearance of MPM2 (a specific mitotic marker), and is associated with upregulation of Cyclin B1, phosphorylation of Cdc25C, and dephosphorylation of Cdc2. J30 also causes Bcl-2 phosphorylation, cytochrome c translocation, and activation of the caspase-9 and caspase-3 cascades. This suggests that the J30-mediated apoptotic signaling pathway depends on caspases and mitochondria. Finally, we show that oral administration of J30 significantly inhibits tumor growth in NOD/*scid* mice bearing human oral, gastric, and drug resistant xenografts. Together, our results suggest that J30 has potential as a chemotherapeutic agent for treatment of various malignancies.

Introduction

One of the most successful classes of anti-tumor drugs targets microtubules, principal components of the cytoskeleton that are important in cell division, organelle transport, cytokinesis, maintenance of cell morphology, and signal transduction (Jordan and Wilson, 2004). There are two categories of antitubulin compounds used to target highly proliferating malignant cells. The microtubule depolymerizing agents, such as vinca alkaloids and colchicinoids, inhibit tubulin polymerization. The microtubule polymerizing agents, such as taxanes and epothilones, promote or stabilize the tubulin polymer form (Pellegrini and Budman, 2005). Recent studies suggest that the inhibitory effects of these drugs are due to their interruption of microtubule dynamics, rather than alteration of microtubule polymer mass. The disruption of microtubule dynamics leads to arrest of growing cells in metaphase/anaphase, causing apoptotic cell death or nonapoptotic slow cell death (Mollinedo and Gajate, 2003).

Taxanes and vinca alkaloids have been in clinical use for a long time, but these drugs have many drawbacks (Attard et al., 2006). First, drug resistance, caused by mutations and/or expression of different tubulin isotypes, limits the widespread use of anti-tubulin agents. Drug resistance may also be caused by overexpression of drug efflux pumps, including the multidrug resistant P-glycoprotein (MDR/Pgp) or multidrug resistance-associated protein (MRP). Second, most drugs (e.g., paclitaxel) in clinical use require intravenous injection with long-term remedial course, causing patients to suffer mentally and physically and reducing the patients' quality of life. Third, although taxanes are effective against ovarian, lung, breast, bladder, and haematological cancers, they are ineffective against solid tumors like gastric, liver, and colorectal carcinomas. Fourth, peripheral neuropathy is a common adverse effect of anti-tubulin drugs, and this limits the tolerable dose. Many researchers are currently working to develop new antitubulin drugs that are

less vulnerable to resistance, can be given orally, have broad spectrum efficiency, and cause minimal neurotoxicity (Bacher et al., 2001; Kuo et al., 2004; Aneja et al., 2006a; Beckers et al., 2002; Tahir et al., 2003; Aneja et al., 2006b).

The sulfonamides have been in clinical use for several decades. Different classes of sulfonamides have antibacterial, diuretic, antidiabetic, antithyroid, antihypertensive, or antiviral activities (Drews, 2000). Recently, many structurally novel sulfonamide derivatives have shown substantial antitumor activity (Scozzafava et al., 2003). For instance, HMN-214 arrests cells in the G2/M phase and exhibits antitumor activity. The antitumor activity is mediated by cytotoxicity, via polo-like kinase disturbance, and by MDR1 downregulation, via binding to the B-subunit of the essential transcription factor NF-Y (Tanaka et al., 2003). Two other sulfonamides, E7070 and E7010, are regarded as a breakthrough in the discovery of new sulfonamides with strong antineoplastic ability (Yoshino et al., 1992; Owa et al., 1999). E7070 is in a class of novel cell cycle inhibitors that block cell cycle progression at multiple points, although its target mechanism remains unclear (Van et al., 2002). E7010 reversibly binds to the colchicine-binding site of tubulin and arrests cells in mitotic phase (Yoshimatsu et al., 1997). Both compounds display antitumor activity against rodent and human tumor xenografts and are currently undergoing phase I/II clinical trials (Smyth et al., 2005; Fox et al., 2006).

We have synthesized a new class of 7-aroylaminoindoline-1- benzene-sulfonamides, and screened them for their ability to inhibit tumor cell growth (Chang et al., 2006). We found one of these novel compounds, N-[1-(4-Methoxy-benzenesulfonyl)-2,3-dihydro-1H-indol-7-yl]-isonicotinamide, namely J30 (Fig1), shows strong antiproliferative activity against human tumor cell lines, as well as the ability that overcomes drug resistance, and of notably, it is orally bioavailable. The purpose of this study is to evaluate the molecular mechanism of J30, to

JPET Fast Forward. Published on July 27, 2007 as DOI: 10.1124/jpet.107.126680
This article has not been copyedited and formatted. The final version may differ from this version.

investigate the effects of J30 on cellular signaling pathways and trigger of apoptosis, and to examine the antitumor efficacy *in vivo*.

Materials and Methods

Chemicals and Antibodies. Camptothecin (CPT), colchicine, etoposide (VP16), paclitaxel (Taxol), and vincristine were purchased from Sigma Chemical Co. (St. Louis, MO). Antibodies were obtained from following companies: α-tubulin (Sigma), Bcl2, Cdc2, Cdc25C, cyclin B1, cytochrome c, and horseradish peroxidase (HRP)-conjugated secondary antibody (Santa Cruz Biotechnology, Inc., Santa Cruz, CA), phosphospecific MPM-2 (Upstate Biotechnology, Lake Placid, NY), COX IV (Cell Signaling Technology, Beverly, MA), PARP (Severigen, Gaithersburg, MD), and fluorescent isothiocyanate (FITC)-conjugated secondary antibody (Ancell Corporation, Bayport, MN). Medium and reagents of cell culture were acquired from Invitrogen (Carlsbad, CA). Microtubule-associated protein (MAP)-rich tubulin and biotin-labeled tubulin were from Cytoskeleton, Inc. (Denver, CO). [^{3}H]colchicine, [^{3}H]paclitaxel, [^{3}H]vinblastine and streptavidin-labeled poly(vinyl toluene) scintillation proximity assay (SPA) beads were purchased from Amersham Pharmacia Biotech (Piscataway, NJ). Other chemicals not specified were from Sigma or Merck (Darmstadt, Germany) with standard analytical or higher grade.

Cell Cultures. Human cancer cell lines (A498, KB, MKN45, HT29, HONE1, H460, DBTRG, TSGH, and Hep3B) used in this study were procured from American Type Culture Collection (ATCC, Rockville, MD) and grown in Dulbecco's modified Eagle's medium, minimal essential medium, or RPMI 1640 medium. Resistant cell lines KB-Vin10, KB-7D, KB-S15, and HONE1-CPT30 were maintained in medium containing an additional 10 nM vincristine, 7 μM VP16, 50 nM Taxol, and 100 nM CPT, respectively. All cell cultures were supplemented with

JPET Fast Forward. Published on July 27, 2007 as DOI: 10.1124/jpet.107.126680
This article has not been copyedited and formatted. The final version may differ from this version.

10% fetal bovine serum, 2 μM glutamine, 100 U/ml penicillin, and 100 μg/ml streptomycin and incubated in a humidified atmosphere (95% air and 5% CO_2) at 37°C. KB-Vin10 and KB-S15 were cell lines resistant against vincristine and paclitaxel, respectively, and both overexpressed the MDR drug efflux protein. KB-7D cells were VP16-resistant cells and overexpressed MRP. HONE1-CPT30 cells have a mutation at topoisomerase I (E418K), resulting in camptothecin resistance. All resistant cell lines were incubated in the drug-free medium for 3 days before harvesting for the growth inhibition assay.

Growth Inhibition Assay. *In vitro* growth inhibition was assessed with the methylene blue assay (Finlay et al., 1984). Briefly, exponentially growing cells were seeded into 24-well culture plates at a density of 8000-20000 cells/ml/well (depending on the doubling time of the cell line), and allowed to adhere overnight. Cells were incubated with various concentrations of drugs for 72 h. Then, we measured A_{595} of the resulting solution from 1% N-lauroylsarcosine exaction. The 50% growth inhibition (IC_{50}) was calculated based on the A_{595} of untreated cells (taken as 100%). The values shown are the means and standard errors of at least three independent experiments performed in duplicate.

***In Vitro* Microtubule Polymerization Assay.** This assay was conducted in a 96-well UV microplate, as described previously (Chang et al., 2003). 0.24 mg MAP-rich tubulin was mixed with various concentrations of drugs and incubated at 37°C in 120 μl reaction buffer (100 mM PIPES, pH 6.9, 1.5 mM $MgCl_2$, 1 mM GTP, and 1% (v/v) DMSO). A_{350} was monitored every 30 s for 30 min, using the PowerWave X Microplate Reader (Bio-Tek Instruments, Winooski,VT). The augment in A_{350nm} indicated the increase in tubulin polymerization. 100% polymerization was defined as the AUC of the untreated control. The IC_{50} was defined as the concentration at which microtubule polymerization was inhibited by 50%, calculated using nonlinear regression.

JPET Fast Forward. Published on July 27, 2007 as DOI: 10.1124/jpet.107.126680
This article has not been copyedited and formatted. The final version may differ from this version.

Tubulin Competition-Binding Scintillation Proximity Assay. This assay was performed in a 96 well-plate (Tahir et al., 2000; Tahir et al., 2001; Tahir et al., 2003). Briefly, [^{3}H]colchicine, [^{3}H]paclitaxel, or [^{3}H]vinblastine sulfate (final concentration, 0.08 μM, 0.16 μM, or 0.25 μM, respectively), were mixed with tested compound and special long chain biotin-labeled tubulin (0.5 μg for colchicine and paclitaxel binding assay, and 1.0 μg for vinblastine binding assay), and then incubated in 100 μl reaction buffer (80 mM PIPES pH 6.8, 1 mM EGTA, 10% glycerol, 1 mM $MgCl_2$, and 1 mM GTP) for 2 h at 37°C. Streptavidin-labeled SPA beads (80 μg, 160 μg, and 200 μg for colchicine, paclitaxel, or vinblastine binding assay, respectively) were then added to each reaction mixture. Then the radioactive counts were directly measured by a scintillation counter and the inhibition constant (*Ki*) was calculated using the Cheng-Prusoff equation (Cheng and Prusoff, 1973).

Measurement of *In Vivo* Microtubule Assembly. We used an established method to measure soluble (depolymerized) and assembled (polymerized) tubulin (Blagosklonny et al., 1995). After treatment, KB cells were collected, lysed with 200 μl lysis buffer (20 mM Tris-HCl, pH 6.8, 1 mM $MgCl_2$, 2 mM EGTA, 1 mM PMSF, 1 mM orthovanadate, 0.5% NP-40, and 20 μg/ml proteinase inhibitor aprotinin, leupeptin and pepstatin), and centrifuged at 12,000 *g* at 4°C for 10 min. This yielded soluble tubulin dimers in the supernatant and polymerized microtubules in the pellet. Equal amounts of the two fractions (on a protein basis) were partitioned by SDS-PAGE. Immunoblots were probed with α-tubulin monoclonal antibody and secondary HRP-conjugated antibody. The blots were developed using an Enhanced Chemiluminescence reagent kit (Perkin-Elmer Life and Analytical Sciences, Boston, MA) followed by development on Kodak Bio-MAX MR film (Rochester, NY).

Immunofluorescence Microscopy. Cells attached to poly(L-lysine)-coated coverslips were

JPET Fast Forward. Published on July 27, 2007 as DOI: 10.1124/jpet.107.126680
This article has not been copyedited and formatted. The final version may differ from this version.

treated with drugs for 24 h. Cells were fixed in methanol/acetone (1:1 v/v) at -20°C for 1h and then washed with PBST for 5 min. Nonspecific sites were blocked by incubating with 5% skim milk in PBST for 1h. A mouse monoclonal antibody against α-tubulin was diluted 1:500 in blocking solution and incubated for 2 h. Cells were washed with PBST twice (10 min each) to remove excess antibody and then probed with FITC-conjugated secondary antibody (1:200) for 1 h at room temperature. The images of α-tubulin with FITC staining were captured with an Olympus BX50 fluorescence microscope (Dulles, VA).

Cell Cycle Analysis. Cell cycle progression was monitored using DNA flow cytometry. After drug treatment, cells were trypsinized, washed with PBS and fixed in 80% ethanol at -20°C for 1 h. The fixed cells were stained with 50 μg/ml RNase and 50 μg/ml propidium iodide at room temperature in the dark for 20 min. The DNA content was determined by a fluorescence-activated cell sorting IV flow cytometer (BD Biosciences, Franklin Lakes, NJ). For each analysis, 10,000 cells were counted and the percentage of cells in each phase was calculated using ModFit LT software (Verity Software House, Topsham, ME).

Western Blot Analysis. After treatment, cell pellets were collected and lysed in a buffer (50 mM Tris-HCl, pH 8.0, 150 mM NaCl, 5 mM EDTA, 2 mM DTT, 2 mM Na_3VO_4, 0.25 mM PMSF, 10 mM NaF, 0.5% NP-40, and proteinase inhibitor aprotinin, leupeptin and pepstatin 20 μg/ml each). Lysates were centrifuged at 12,000 *g* for 15 min, and the supernatants were collected and quantified. Equal amounts of lysate (on a protein basis) were then differentiated by SDS-PAGE, blotted on PVDF membranes, conjugated with various specific primary antibodies, and then probed with appropriate secondary antibodies. The immunoreactive bands were detected by the ECL method and visualized on Kodak Bio-MAX MR film.

Apoptosis Studies. The early stages of apoptosis were monitored by Annexin-V-Fluorescein

JPET Fast Forward. Published on July 27, 2007 as DOI: 10.1124/jpet.107.126680
This article has not been copyedited and formatted. The final version may differ from this version.

(apoptotic cell marker) and PI (necrotic cell marker) double staining. The staining method was according to the manufacturer's staining kit (Roche Applied Science, Indianapolis, IN). Cells were analyzed on a FACSVantage flow cytometer (BD Biosciences, Franklin Lakes, NJ), using 488 nm as the excitation wavelength and a 515 nm bandpass filter for detection of fluorescein fluorescence and a 600 nm cutoff filter for detection of PI fluorescence. For each measurement, 10,000 events were measured.

Caspase activity assay. Caspase activities were measured with the fluorometic assay kit (R&D systems Inc., Minneapolis, MN) or the CaspACE Assay System Fluorometric (Promega Corporation, Madison, WI) that detects cleavage of specific fluorogenic peptide substrates. The fluorescence of the cleaved substrate was determined with a Victor 1420 Multilabel Counter (Wallac, Turku, Finland).

Preparation of Mitochondrial and Cytosolic Fractions. Cells were gently homogenized with a Dounce homogenizer in a buffer (20 mM HEPES, pH7.5, 10 mM KCl, 1.5 mM $MgCl_2$, 1 mM EDTA, 1 mM dithiothreitol, 0.5 mM phenylmethylsulfonyl fluoride, 5 μg/ml aprotinin, 50 μg/ml leupeptin, 50 μg/ml pepstatin, and 250 mM sucrose). The homogenate was centrifuged at 750 *g* for 5 min at 4°C to remove unbroken cells and nuclei. Then, the supernatant was centrifuged at 16,000 *g* for 20 min at 4°C. The pellet from this step was saved as the mitochondria fraction and the supernatant was subjected to further ultracentrifugation at 100,000 *g* for 1 h at 4°C, to eliminate trace membrane contamination. The 100,000 *g* supernatant was saved as the cytoplasmic fraction. For immunoblotting, proteins of the two fractions were separated using 12% SDS-PAGE, followed by electroblotting onto PVDF membrane. Cytochrome c was detected by a monoclonal antibody (mAb) at a dilution recommended by the manufacturer (Santa Cruz). Secondary goat anti-mouse horseradish peroxidase (HRP)-labeled antibody was detected by enhanced ECL.

β-actin and COX IV were probed as the internal control of cytosolic and mitochondrial fraction, respectively.

Antitumor activity *in vivo*. The antitumor effect of J30 on human tumor xenografts was examined by s.c. inoculation of 2×10^6 cells in NOD/*scid* mice (purchased from the Laboratory Animal Center of Tzu Chi University, Hualien, Taiwan), fed under specific pathogen–free conditions and provided with sterile food and water *ad libitum*. When tumor volumes reached 100-150 mm^3 (measured with calipers and estimated according to the equation [(major axis) × (minor axis)^2 × 6/π]), animals were assigned into groups randomly and given either vehicle or oral J30 (dissolved in 0.5% methylcellulose in ddH_2O) 5 days/week for 2 weeks. Mouse body weight and tumor volume were measured 3 times per week.

Results

Growth inhibition of J30 against human cancer cell lines. We used the methylene blue assay to evaluate the antiproliferative effect of J30 on human cancer cells from several representative solid tumor cell lines: oral carcinoma (KB), nasopharyngeal carcinoma (HONE1), gastric cancer (TSGH and MKN45), kidney cancer (A498), liver cancer (Hep3B), colon cancer (HT29), lung cancer (H460), and glioblastoma multiforme (DBTRG). All cancer cell lines that we tested showed high susceptibility to J30, with the IC_{50} ranging between 15~20 nM. (Table 1) We further examined the efficacy of J30 against drug-resistant cell lines. Despite the high level of expression of drug resistant efflux protein (MDR/Pgp or MRP) in KB-Vin10, KB-S15, and KB-7D cells, J30 showed similar cytotoxic efficacy between parental and these resistant sub-lines. J30 also displayed potent antigrowth activity against a topoisomerase I-mutant (HONE1-CPT30). (Table 2)

JPET Fast Forward. Published on July 27, 2007 as DOI: 10.1124/jpet.107.126680
This article has not been copyedited and formatted. The final version may differ from this version.

J30 deploymerizes microtubules *in vitro* by binding to the colchicine-binding site. Next, we tested the ability of J30 to depolymerize the pure MAP-rich tubulins *in vitro*. The results (Fig. 2A) show that J30 inhibits polymerization of tubulin in a concentration dependent manner, with an IC_{50} of 0.48 μM. J30 disrupted tubulin assembly almost completely at 2.5 μM. Based on our competition-binding Scintillation Proximity Assay, we conclude that J30 does not reduce the specific SPA counts stimulated by conjugating the biotin-labeled tubulin with [^{3}H]paclitaxel or with [^{3}H]vinblastine, but J30 strongly competes with [^{3}H]colchicine binding to tubulin. The inhibition constant of J30 (Ki, 0.2 μM) was much lower than that of colchicine (Ki, 1.8 μM). (Fig. 2B)

We also studied the effect of J30 on the dynamics of microtubule assembly at the cellular level. As shown in Fig. 3A, the polymerization of tubulin was increased in Taxol-treated cells compared to the control cells. Cells treated with J30 and cells treated with vincristine both showed a decreased amount of the polymer form of tubulin. Next, we used immunoflurorescence microscopy to study the effect of J30 on the microtubule network. Compared to untreated KB controls, cells treated with Taxol produced shorter but denser microtubules (Fig. 3B, top middle) and cells treated with vincristine displayed a destroyed filament-like structure and reduced the microtubule extent (Fig. 3B, top right). J30 caused changes similar to those of vincristine, in that the microtubule network shrank significantly at 20 nM and was disrupted thoroughly at 40 nM.

J30 arrests the cell cycle in G2/M phase by consecutive activation of Cdc2/Cyclin B1. We treated KB cells with varying concentrations of J30 for 24h or a single concentration for 6-48 h to determine the influence of J30 on the cell cycle. The results (Fig. 4A) indicate that J30 caused collapse at the G1 phase, causing a dramatic increase in the number of cells in the G2/M phase. While the concentration was up to 40 nM, the percentage of cell numbers at G2/M reached plateau.

When the cells were treated with a higher concentration of J30, the cells in the G2/M cell stayed nearly the same and the subG1 population, which had less than diploid DNA content (indicative of apoptosis), increased slightly. Microtubule-inhibiting agents induce cell cycle arrest in the G2/M phase and then trigger apoptosis. Thus, we performed Annexin V/PI double staining in J30-treated cells to monitor the phosphatidylserine exposure, a signal of early apoptosis. The populations of early apoptotic cells (Annexin V+/PI -) and late apoptotic cells (Annexin V+/PI+) increased dramatically in a concentration dependent manner following 24 h treatment with J30 (from 0.39 % to 52.9 %, right bottom; and 0.3 % to 17.66 %, right top) (Fig. 4B).

Next, we examined the signaling transduction pathway of G2/M arrest evoked by J30 treatment in KB cells by using immunoblotting analysis. As shown in Figure 4C and D, exposures to J30 (concentration of 40 nM for 24 h) caused an excessive elevation on the amount of MPM2 phospho-epitope. The protein level gradually accumulated from 6 to 24h in a time-dependent manner and coincided with the accumulation of cells in the G2/M phase. Activation of protein phosphatase Cdc25C became evident at 12 h with the emergence of a defined phosphorylated form. Cdc2 kinase, the downstream substrate of Cdc25C, was dephosphorylated at 24 h. Likewise, the quantity of cyclin B1 showed an increase at J30 concentrations of 20-160 nM (24 h treatment). The increase was observed as early as at 6 h, and the upregulation was maintained at least until 24 h.

J30 causes apoptosis through caspase activation, Bcl2 dephosphorylation, and cytochrome c translocation. We assessed the activity of caspase 3 and caspase 9 with their flourogenic tetrapeptide substrates (Fig. 5A) to determine the mechanism of apoptosis. The enzymatic activities of caspase 3 and caspase 9 rose simultaneously following treatment of KB cells with J30, reaching maxima (5.3 and 6.5 fold compared to the controls, respectively) at 36 h. Our results also show that cleavage of Poly (ADP-ribose) polymerase (PARP), a well-known

substrate for caspase 3 cleavage that forms an 85 kDa fragment (Nicholson, et al., 1995), appeared after the concentration of J30 exceeded 40 nM (Fig. 5B), and was concomitant with the raise of caspase 3 activity at 18 h (Fig. 5C). We also monitored cytochrome c translocation, a major event in mitochondria-mediated apoptosis. J30 induced a time dependent translocation of cytochrome c from the mitochondria to the cytosol (Fig. 5D), as was coincided with the appearance of the inactive phosphorylated form of Bcl2, which lost the guardian ability of mitochondria integrity (Fig. 5B and C).

Efficacy of oral J30 in xenograft mice. Next, we determined whether oral administration of J30 was effective against human tumors implanted in NOCD/*scid* mice. Figure 6A and B show that J30 inhibits tumor growth in a dose dependent manner in KB and MKN45 xenograft mice. For KB, oral administration of J30 at 15 and 20 mg/kg (5 days/week) for 2 weeks caused tumor suppression of 31% and 49% respectively (compared with controls) on day 26. We found a similar pattern of inhibition in MKN45-bearing mice, where the tumor growth inhibitions were 27% at 15 mg/kg and 48% at 20 mg/kg on day 28. In addition, we examined J30's ability against the KB-Vin10 xenograft tumor, which is resistant to vincristine. We found that oral J30 exhibited significant antitumor activity against vincristine-resistant cells as well (41%, Fig 6C). In these animal models, we observed no significant morbidity and a body weight loss <10%. These data clearly show that oral J30 effectively inhibits tumor growth in an *in vivo* murine model.

Discussion

The microtubules are an attractive target for chemotherapeutic agents. This paper presents experiments with a novel compound, J30, originally identified as the lead compound (from studies of structure-activity-relationships) of a novel class of indoline-sulfonamide derivatives (Chang et

al., 2006). Its predicted effectiveness is based on the structural analogue of typical indoline agents that are known to depolymerize microtubules. Our results show that J30 has broad spectrum ability, at the nanomolar range, to inhibit growth of various cancer cell lines, as well as drug resistant sub-lines (Table 1 and 2). Notably, it is more potent than any other sulfonamide derivatives reported to date (Scozzafava et al., 2003). Drug resistance is a serious problem that restricts the use of microtubule-interfering drugs for clinical therapy. J30 exerts a similar potency, regardless of the cell's MDR or MRP status (Table 2), suggesting that it is not a substrate of these efflux pumps. Moreover, J30 is also effective against cell lines that are resistant to other remedially used drugs, such as CPT and oxaliplatin (data not shown). However, whether J30 overcomes resistance induced by tubulin mutations and/or different isoptype expressions still needs to be verified.

To clarify the molecular targets of J30, we examined whether it targets microtubules. Our data clearly demonstrate that J30 strongly depolymerizes microtubules by binding to the colchicine-binding site with a high affinity than colchicine itself. Western blot and immunofluorescence microscopy, using the anti α-tubulin antibody, confirm that J30 deploymerizes microtubules and degrades the microtubule network in living cells. Like other agents that target microtubules, J30 induces a concentration and time dependent G2/M blockade, as indicated by flow analysis and expression of the MPM2 epitope, a mitosis-specific marker (Fig. 4C and D). Regulation of Cdc2 activity is controlled by Cyclin B1 binding, phosphorylation of Thr161, and dephosphorylation of Tyr14 and Tyr15 by Cdc25C (Norbury and Nurse, 1992). Cdc25C itself is highly regulated by phosphorylation (Hutchins and Clarke, 2004). Blocking any of these steps may lead to cell cycle arrest and subsequent apoptosis. In this study, we found that treatment with 40 nM J30 for 24 h induces Cdc25C phosphorylation, abnormal Cyclin B1 accumulation, and Cdc2 dephosphorylation, and cell cycle arrest in the mitotic phase. J30 causes

an early accumulation of Cyclin B1, similar with other's observation on Taxol-treated cells (Ling et al., 1998). We also noticed that Cdc25C phosphorylation (which starts 6 h after J30 administration) precedes the appearance of Cdc2 dephosphorylation (first seen at 24 h after J30 administration). It would be probably due to the complex multiple post-translational regulations of Cdc25C (Perdiguero and Nebreda, 2004). Taken together, these data suggest that J30 induces cell cycle arrest in the G2/M phase via constitutive activation of Cdc2/Cyclin B1.

It is widely accepted that microtubule-interfering agents cause apoptosis by causing cell cycle arrest (Mollinedo and Gajate, 2003). In addition to the effect of J30 on the cell cycle, we found that it also provokes apoptosis, as indicated by an increase in subG1 population and Annexin V positivity (Fig. 4A and B). Apoptotic signaling involves activation of intracellular caspases. Our results show that J30 increases the activity of caspase 9 and caspase3. Caspases are activated during apoptosis by two important pathways: (1) cross-linking of "death receptors" following extrinsic triggering and (2) release of apoptogenic factors from mitochondria following intrinsic signals (Chipuk and Green, 2005). Our results show that J30 evokes Bcl2 hyperphosphorylation, losing its protective ability to maintain the mitochondrial membrane potential and permeability, and subsequently resulting in the release of proapoptotic protein cytochrome c into cytosol. While cytosolic cytochrome c meets procaspase 9, the apoptosome is formed, and in turn activates the downstream executioner caspase 3 that induces PARP cleavage. Therefore we hypothesize that J30 triggers apoptosis via the intrinsic mitochondrial pathway.

Finally, we demonstrate that oral administration of J30 has significant therapeutic efficacy against human cervical (KB), gastric (MKN45), and drug resistant (KB-Vin10) tumor xenografts in mice (Fig. 6). We observed no significant body weight loss during these experiments, suggesting that J30 may have insignificant side effects. Clearly, we must perform more detailed

experiments to develop an optimal protocol for J30 administration. In addition to overcoming drug resistance *in vivo*, and distinct from several microtubule-interfering drugs used in cancer chemotherapy by intravenous injection (Mollinedo and Gajate, 2003), oral administration of J30 allows assessment of the benefits of chronic remedial regimens.

In conclusion, our data provide compelling evidence that the novel sulfonamide-based compound, J30, has broad-spectrum efficacy *in vitro* by triggering apoptosis and is effective against tumor xenografts in murine models. In addition, J30 is less vulnerable to drug resistance, at least caused by MDR or MRP overexpression, and is effective when administered orally to mice. Our study indicates that J30 has potential as an anti-neoplastic drug for oral treatment of various malignancies and drug resistant tumors.

References

Aneja R, Lopus M, Zhou J, Vangapandu SN, Ghaleb A, Yao J, Nettles JH, Zhou B, Gupta M, Panda D, Chandra R and Joshi HC (2006a) Rational design of the microtubule-targeting anti-breast cancer drug EM015. *Cancer Res* **66**:3782-3791.

Aneja R, Zhou J, Vangapandu SN, Zhou B, Chandra R and Joshi HC (2006b) Drug-resistant T-lymphoid tumors undergo apoptosis selectively in response to an antimicrotubule agent, EM011. *Blood* **107**:2486-2492.

Attard G, Greystoke A, Kaye S and De BJ (2006) Update on tubulin-binding agents. *Pathol Biol (Paris)* **54**:72-84.

Bacher G, Nickel B, Emig P, Vanhoefer U, Seeber S, Shandra A, Klenner T and Beckers T (2001) D-24851, a novel synthetic microtubule inhibitor, exerts curative antitumoral activity in vivo, shows efficacy toward multidrug-resistant tumor cells, and lacks neurotoxicity. *Cancer Res* **61**:392-399.

Beckers T, Reissmann T, Schmidt M, Burger AM, Fiebig HH, Vanhoefer U, Pongratz H, Hufsky H, Hockemeyer J, Frieser M and Mahboobi S (2002) 2-aroylindoles, a novel class of potent, orally active small molecule tubulin inhibitors. *Cancer Res* **62**:3113-3119.

Blagosklonny MV, Schulte TW, Nguyen P, Mimnaugh EG, Trepel J and Neckers L (1995) Taxol induction of p21WAF1 and p53 requires c-raf-1. *Cancer Res* **55**:4623-4626.

Chang JY, Hsieh HP, Chang CY, Hsu KS, Chiang YF, Chen CM, Kuo CC and Liou JP (2006)

7-Aroyl-aminoindoline-1-sulfonamides as a novel class of potent antitubulin agents. *J Med Chem* **49**:6656-6659.

Chang JY, Hsieh HP, Pan WY, Liou JP, Bey SJ, Chen LT, Liu JF and Song JS (2003) Dual inhibition of topoisomerase I and tubulin polymerization by BPR0Y007, a novel cytotoxic agent. *Biochem Pharmacol* **65**:2009-2019.

Cheng Y and Prusoff WH (1973) Relationship between the inhibition constant (K1) and the concentration of inhibitor which causes 50 per cent inhibition (I50) of an enzymatic reaction. *Biochem Pharmacol* **22**:3099-3108.

Chipuk JE and Green DR (2005) Do inducers of apoptosis trigger caspase-independent cell death? *Nat Rev Mol Cell Biol* **6**:268-275.

Drews J (2000) Drug discovery: a historical perspective. *Science* **287**:1960-1964.

Finlay GJ, Baguley BC and Wilson WR (1984) A semiautomated microculture method for investigating growth inhibitory effects of cytotoxic compounds on exponentially growing carcinoma cells. *Anal Biochem* **139**:272-277.

Fox E, Maris JM, Widemann BC, Meek K, Goodwin A, Goodspeed W, Kromplewski M, Fouts ME, Medina D, Cho SY, Cohn SL, Krivoshik A, Hagey AE, Adamson PC and Balis FM (2006) A phase 1 study of ABT-751, an orally bioavailable tubulin inhibitor, administered daily for 7 days every 21 days in pediatric patients with solid tumors. *Clin Cancer Res* **12**:4882-4887.

Hutchins JR and Clarke PR (2004) Many fingers on the mitotic trigger: post-translational regulation of the Cdc25C phosphatase. *Cell Cycle* **3**:41-45.

Jordan MA and Wilson L (2004) Microtubules as a target for anticancer drugs. *Nat Rev Cancer* **4**:253-265.

Kuo CC, Hsieh HP, Pan WY, Chen CP, Liou JP, Lee SJ, Chang YL, Chen LT, Chen CT and Chang JY (2004) BPR0L075, a novel synthetic indole compound with antimitotic activity in human cancer cells, exerts effective antitumoral activity in vivo. *Cancer Res* **64**:4621-4628.

Ling YH, Tornos C and Perez-Soler R (1998) Phosphorylation of Bcl-2 is a marker of M phase events and not a determinant of apoptosis. *J Biol Chem* **273**:18984-18991.

Mollinedo F and Gajate C (2003) Microtubules, microtubule-interfering agents and apoptosis. *Apoptosis* **8**:413-450.

Nicholson DW, Ali A, Thornberry NA, Vaillancourt JP, Ding CK, Gallant M, Gareau Y, Griffin PR, Labelle M and Lazebnik YA (1995) Identification and inhibition of the ICE/CED-3 protease necessary for mammalian apoptosis. *Nature* **376**:37-43.

Norbury C and Nurse P (1992) Animal cell cycles and their control. *Annu Rev Biochem* **61**:441-470.

Owa T, Yoshino H, Okauchi T, Yoshimatsu K, Ozawa Y, Sugi NH, Nagasu T, Koyanagi N and Kitoh K (1999) Discovery of novel antitumor sulfonamides targeting G1 phase of the cell cycle. *J Med Chem* **42**:3789-3799.

Pellegrini F and Budman DR (2005) Review: tubulin function, action of antitubulin drugs, and new drug development. *Cancer Invest* **23**:264-273.

Perdiguero E and Nebreda AR (2004) Regulation of Cdc25C activity during the meiotic G2/M

transition. *Cell Cycle* **3**:733-737.

Scozzafava A, Owa T, Mastrolorenzo A and Supuran CT (2003) Anticancer and antiviral sulfonamides. *Curr Med Chem* **10**:925-953.

Smyth JF, Aamdal S, Awada A, Dittrich C, Caponigro F, Schoffski P, Gore M, Lesimple T, Djurasinovic N, Baron B, Ravic M, Fumoleau P and Punt CJ (2005) Phase II study of E7070 in patients with metastatic melanoma. *Ann Oncol* **16**:158-161.

Tahir SK, Han EK, Credo B, Jae HS, Pietenpol JA, Scatena CD, Wu-Wong JR, Frost D, Sham H, Rosenberg SH and Ng SC (2001) A-204197, a new tubulin-binding agent with antimitotic activity in tumor cell lines resistant to known microtubule inhibitors. *Cancer Res* **61**:5480-5485.

Tahir SK, Kovar P, Rosenberg SH and Ng SC (2000) Rapid colchicine competition-binding scintillation proximity assay using biotin-labeled tubulin. *Biotechniques* **29**:156-160.

Tahir SK, Nukkala MA, Zielinski Mozny NA, Credo RB, Warner RB, Li Q, Woods KW, Claiborne A, Gwaltney SL, Frost DJ, Sham HL, Rosenberg SH and Ng SC (2003) Biological activity of A-289099: an orally active tubulin-binding indolyloxazoline derivative. *Mol Cancer Ther* **2**:227-233.

Tanaka H, Ohshima N, Ikenoya M, Komori K, Katoh F and Hidaka H (2003) HMN-176, an active metabolite of the synthetic antitumor agent HMN-214, restores chemosensitivity to multidrug-resistant cells by targeting the transcription factor NF-Y. *Cancer Res* **63**:6942-6947.

Van KC, Beijnen JH and Schellens JH (2002) E7070: a novel synthetic sulfonamide targeting the

cell cycle progression for the treatment of cancer. *Anticancer Drugs* **13**:989-997.

Yoshimatsu K, Yamaguchi A, Yoshino H, Koyanagi N and Kitoh K (1997) Mechanism of action of E7010, an orally active sulfonamide antitumor agent: inhibition of mitosis by binding to the colchicine site of tubulin. *Cancer Res* **57**:3208-3213.

Yoshino H, Ueda N, Niijima J, Sugumi H, Kotake Y, Koyanagi N, Yoshimatsu K, Asada M, Watanabe T and Nagasu T (1992) Novel sulfonamides as potential, systemically active antitumor agents. *J Med Chem* **35**:2496-2497.

Footnotes

The first two authors contribute equally.

This work was supported in part by grants from National Health Research Institutes, Taipei, Taiwan (NHRI intramural grant CA-095-PP-04), and the National Science Council, Taipei, Taiwan (NSC 95-2752-B-400-001-PAE).

Reprint requests: Dr. Jang-Yang Chang, National Institute of Cancer Research, National Health Research Institutes, 7th Floor, No.161, Section 6, Ming-Chuan East Road, Taipei 114, Taiwan, R.O.C., E-mail: jychang@nhri.org.tw.

Legends for Figures

Figure 1. Chemical structure of J30.

Figure 2. J30 deploymerizes microtubule *in vitro* by binding to the colchicine-binding site. A, Effect of J30 on *in vitro* tubulin polymerization. MAP-rich tubulins were incubated at 37°C with absence (DMSO control) or presence of drugs (colchicine or serial concentrations of J30). Absorbance at 350 nm was measured every 30 s for 30 min, and presented as the increased polymerized microtubule. B, The binding site of J30 on tubulin was examined by using competition-binding scintillation proximity assay, as described in *Materials and Methods*. The 100% binding represented [^{3}H]ligand bound of control group without tested compounds. Double-reciprocal plot indicated that J30 was a competitive inhibitor to colchicine-binding site on tubulin. Each data point, the mean ± SD.

Figure 3. A, J30 affects the dynamics of microtubule assembly toward depolymerization *in vivo*. KB cells were exposed to different compounds for 24 h. Cell pellets were lysed with lysis buffer (20 mM Tris-HCl, pH 6.8, 1 mM $MgCl_2$, 2 mM EGTA, 1 mM PMSF, 1 mM orthovanadate, 0.5% NP-40, and 20 μg/ml proteinase inhibitor aprotinin, leupeptin and pepstatin). The polymer and free form of tubulins were separated by centrifugation at 12,000 *g* at 4°C for 15 min, followed by SDS-PAGE electrophoresis and α-tubulin immunoblotting. B, Immunohistochemistry of KB cells treated with 0.5 nM vincristine, 10 nM Taxol, or different concentrations of J30 for 24 h. Cells were fixed, labeled with FITC-conjugated mouse anti-tubulin antibody, and observed by Olympus-BX50 fluorescence microscope.

JPET Fast Forward. Published on July 27, 2007 as DOI: 10.1124/jpet.107.126680
This article has not been copyedited and formatted. The final version may differ from this version.

Figure 4. J30 causes cell cycle arrest at G2/M phase via activating the mitotic regulators, and subsequently induces cell apoptosis. A, The concentration (left panel; treatment for 24 h) and time (right panel; treatment with 40 nM) effect of J30 on cell cycle progressions of KB cells, using PI staining via flow cytometric analysis. B, Annexin-V-Fluorescein (FL-1)/PI (FL-2) double staining of KB cells exposed to different concentrations of J30 for 24 h. The Annexin V–/PI – represented viable cells (left bottom); Annexin V+/PI – indicated early apoptotic cells (right bottom); Annexin V+/PI + indicated late apoptotic cells (right top). Panel C and D showed the influence of J30 on change of expressed and phosphorylated level of key mitotic regulators. C, KB cells treated with various concentrations of J30 for 24h. D, KB cells treated with 40 nM J30 for different times.

Figure 5. J30 induces caspase activations, downstream PARP cleavage, Bcl2 dephosphorylation and cytocrome c release. A, Time course analysis of caspase enzyme activities induced by J30. The enzyme activities were determined by using Ac-DEVD-AMC (caspase-3 substrate) and LEHD-AFC (caspase-9 substrate) fluorogenic substrates. The relative activity unit was expressed as the ratio of experimental sample to control (without drug treatment). Panel B and C indicated the effect of J30 on Bcl2 dephosphrylation and PARP cleavage. B, KB cells treated with various concentrations of J30 for 24h. C, KB cells treated with 40 nM J30 for different times. D, Relocation of cytochrome c following J30 treatment. At 0, 12, 18, and 24 h of 40 nM J30 treatment, KB cells were fractionated into the cytosolic and mitochondrial fractions, as described in *Materials and Methods*. 20 μg protein samples were separated by SDS-PAGE for immunoblot analysis using antibody against and cytochrome c. β-Actin and COX IV were stained as the internal control of cytosolic and mitochondrial fractions, respectively.

JPET Fast Forward. Published on July 27, 2007 as DOI: 10.1124/jpet.107.126680
This article has not been copyedited and formatted. The final version may differ from this version.

Figure 6. *In vivo* antitumor activity of J30 in human A, oral (KB), B, gastric (MKN45) and C, drug-resistant (KB-Vin10) xenograft models. After tumor size reached 100~150 mm^3, mice received *p.o.* administration of 0, 15, or 20 mg/kg of J30 5 days/week for 2 consecutive weeks [QD5(2) x 2]. In KB-Vin10 bearing mice, vincristine (1mg/kg) was *i.v.* administered once/week for 2 weeks [QD1(6) × 2] as the negative control. Tumor size and body weight were measured 3 times/week. The body weight was shown as the percentage of that on the day of first administration.

JPET Fast Forward. Published on July 27, 2007 as DOI: 10.1124/jpet.107.126680
This article has not been copyedited and formatted. The final version may differ from this version.

Table 1. Growth inhibition of J30 against various human cancer cell lines

Origin	Cell Lines	IC_{50} (nM)[a]
Cervical carcinoma	KB[b]	19.3 ± 5.8
Nasopharyngeal carcinoma	HONE1	15.7 ± 0.9
Gastric carcinoma	TSGH	21.3 ± 6.1
Gastric carcinoma	MKN45	20.2 ± 6.6
Kidney carcinoma	A498	16.1 ± 0.1
Hepatocellular carcinoma	Hep3B	18.2 ± 0.4
Colorectal carcinoma	HT29	16.2 ± 1.2
Non-small-cell lung carcinoma	H460	22.5 ± 8.5
Glioblastoma	DBTRG	21.0 ± 5.6

[a] Each value represented the mean ± S.D. of three independent experiments.

[b] The KB cell line was originally derived from an epidermal carcinoma of the mouth but has now been shown to have HeLa characteristics.

Table 2. Growth inhibition of J30 against drug-resistant cell lines[a]

Cell Lines	Resistant Type	IC50 [b]				
		Vincristine (nM)	VP16 (μM)	Taxol (nM)	CPT (nM)	J30 (nM)
KB	Parental	0.4 ± 0.1	1.1 ± 0.2	3.3 ± 1.2	43.3 ± 2.4	19.3 ± 5.8
KB-Vin10	MDR ↑	90.1 ± 7.4	23 ± 3	16500 ± 707	280 ± 36	17.4 ± 5.1
KB-7D	MRP ↑	1.2 ± 0.4	54 ± 3.5	7.9 ± 0.5	133 ± 16	7.2 ± 0.6
KB-S15	MDR ↑	17.6 ± 2.2	3.5 ± 0.3	273 ± 15	55.7 ± 5.9	15.1 ± 2.9
HONE1	Parental	1.4 ± 0.3	0.5 ± 0.1	2.7 ± 0.4	27 ± 5	15.7 ± 0.9
HONE1-CPT30	TOP 1 mutant	1.6 ± 0.2	0.4 ± 0.1	2.8 ± 0.6	355 ± 30	16.0 ± 0.7

[a] All resistant cell lines are maintained in drug-free medium for 3 days before seeding for growth inhibition assay.

[b] Each value represented the mean ± S.D. of three independent experiments.

Figure 1

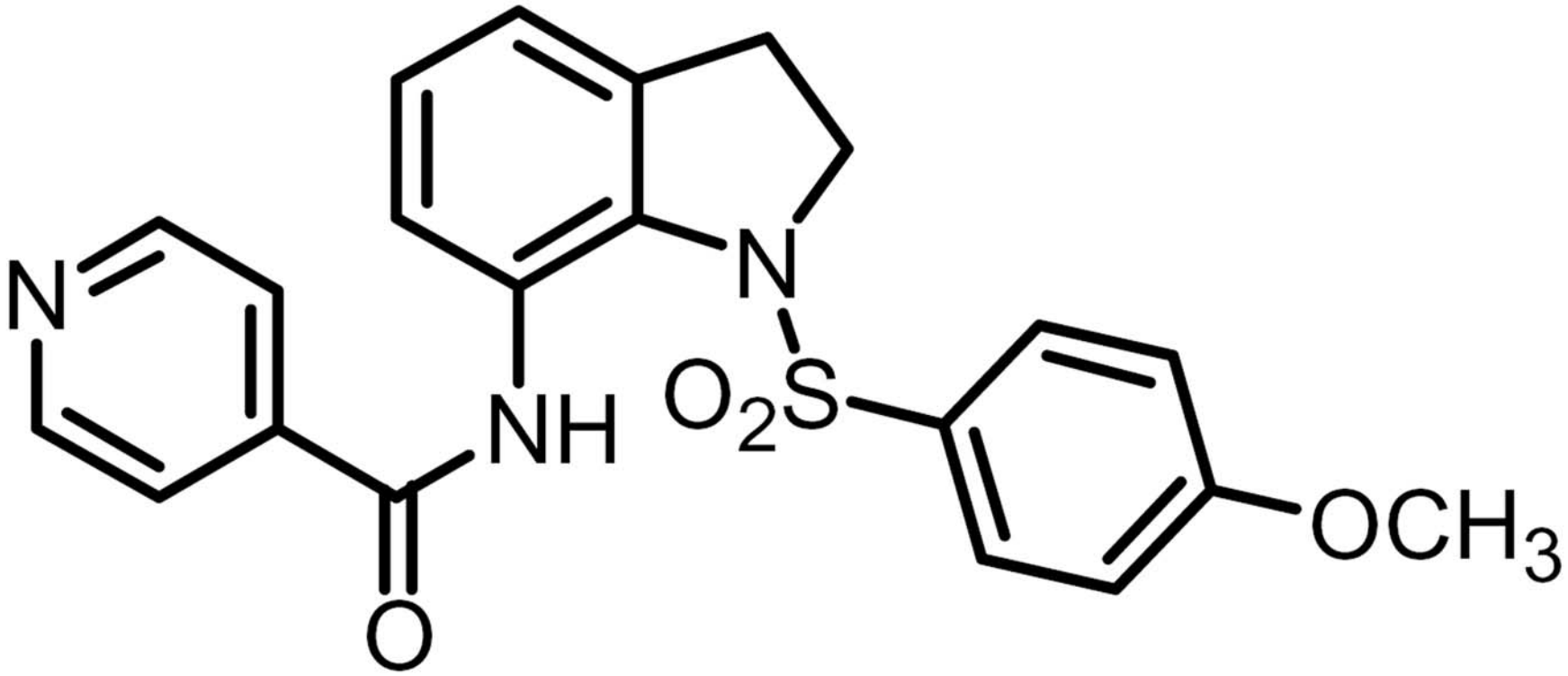

Figure 2A

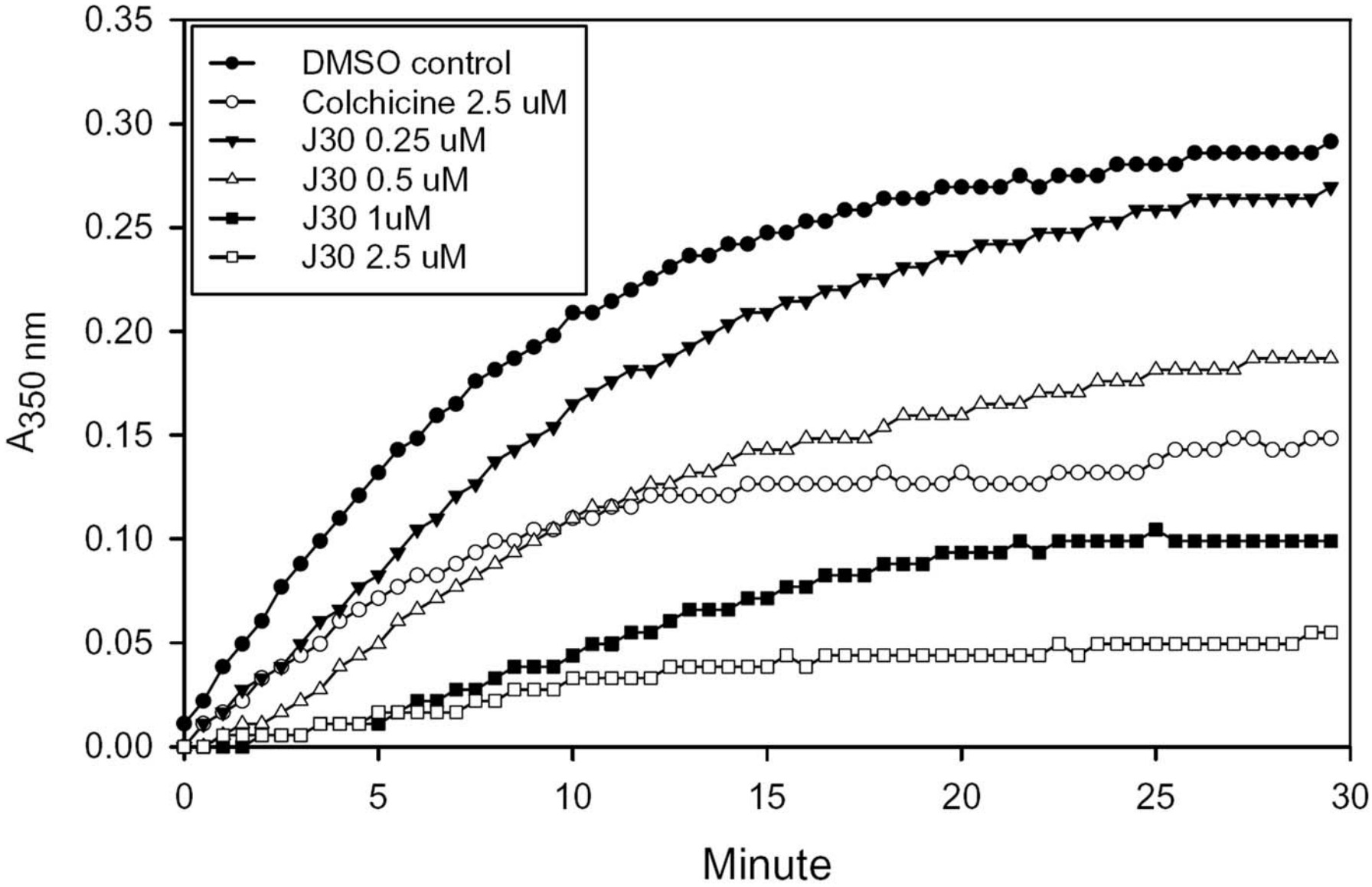

Figure 2B

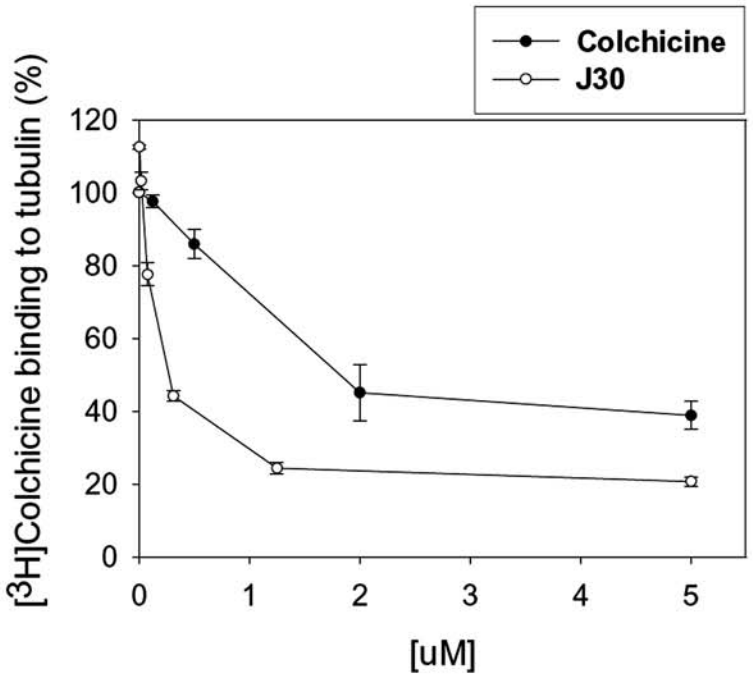

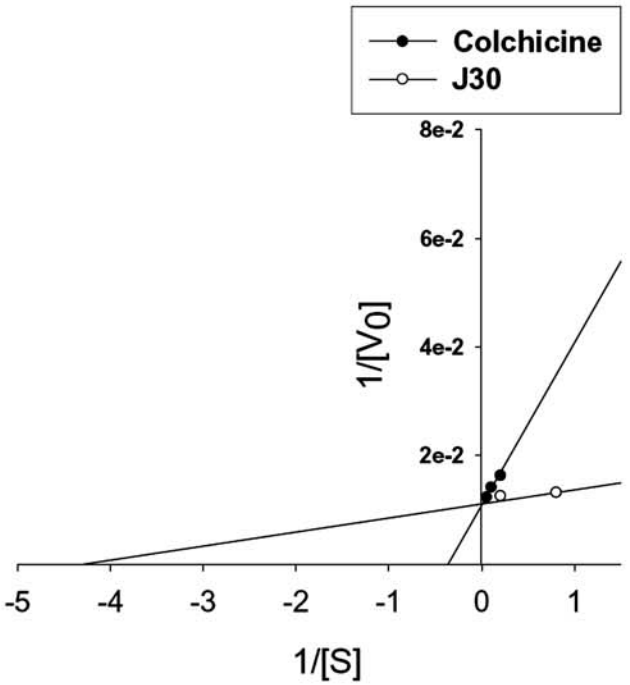

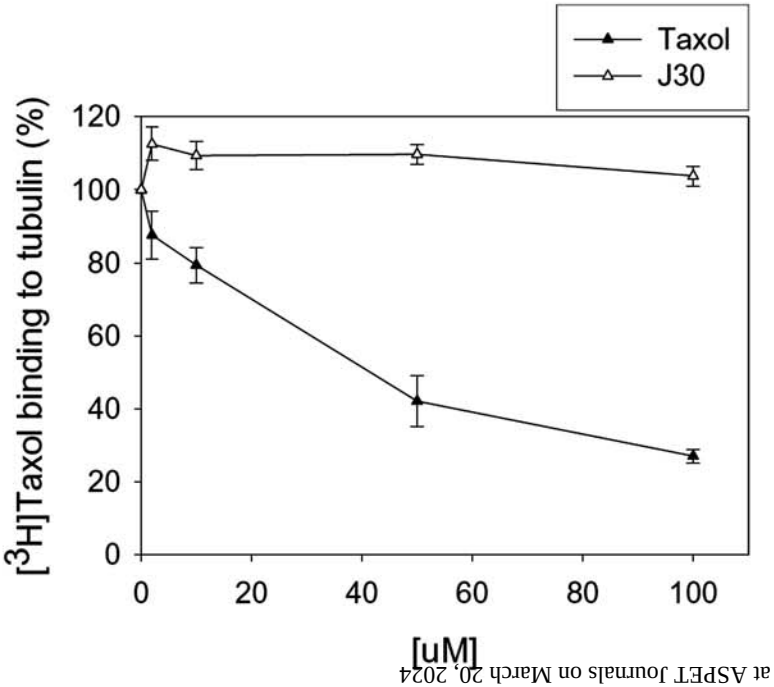

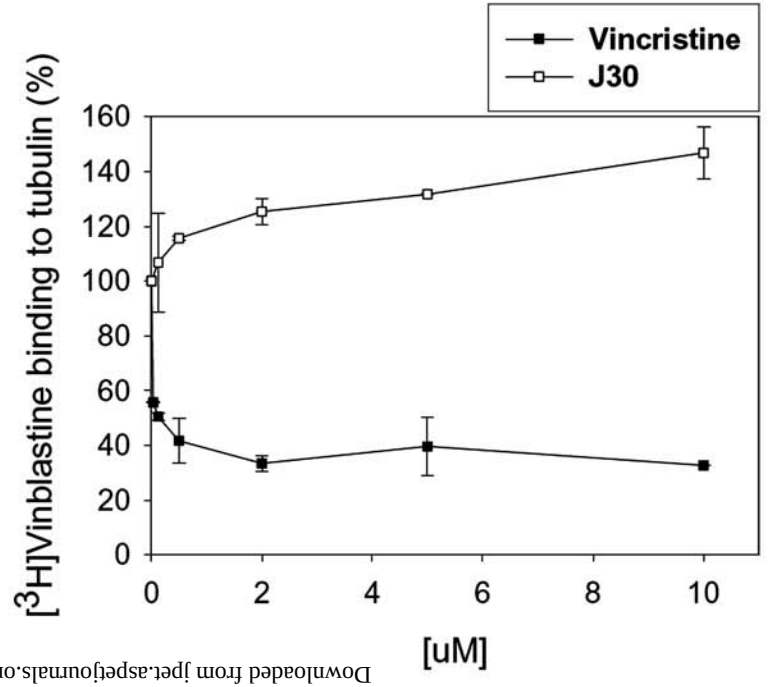

Figure 3A

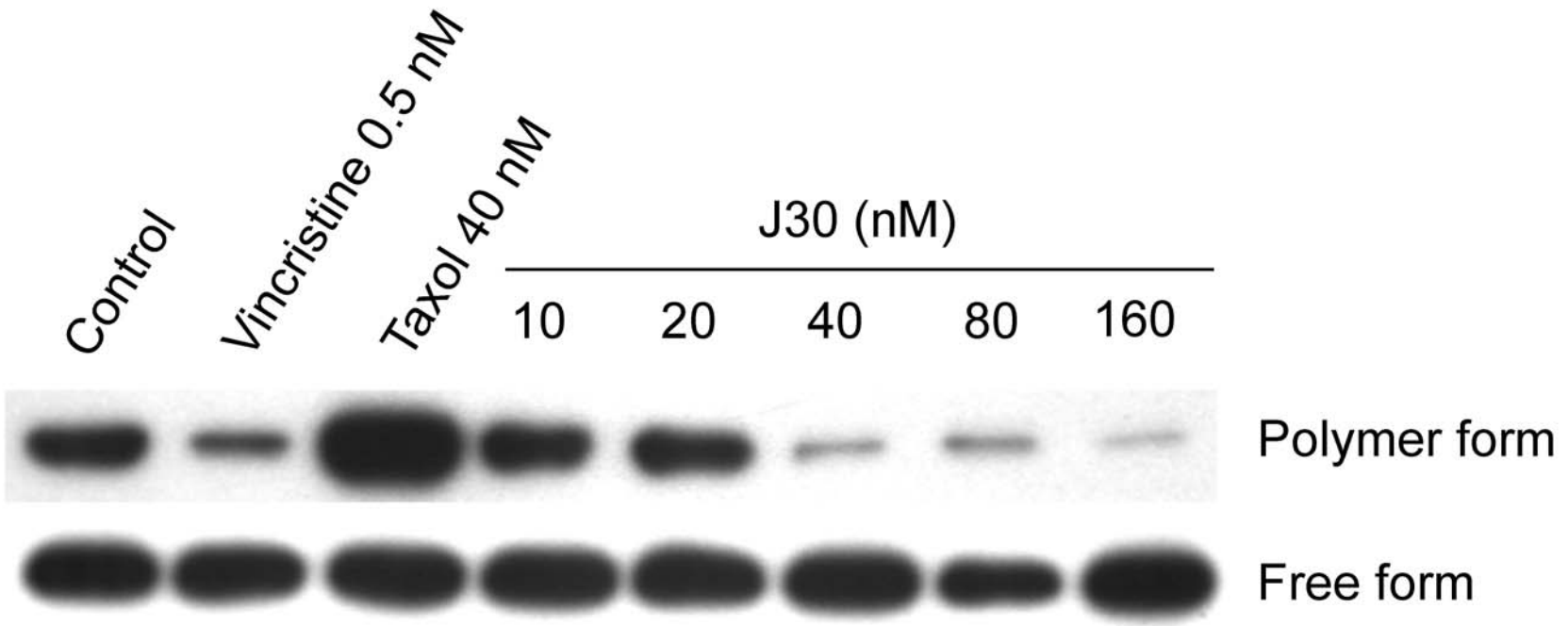

Figure 3B

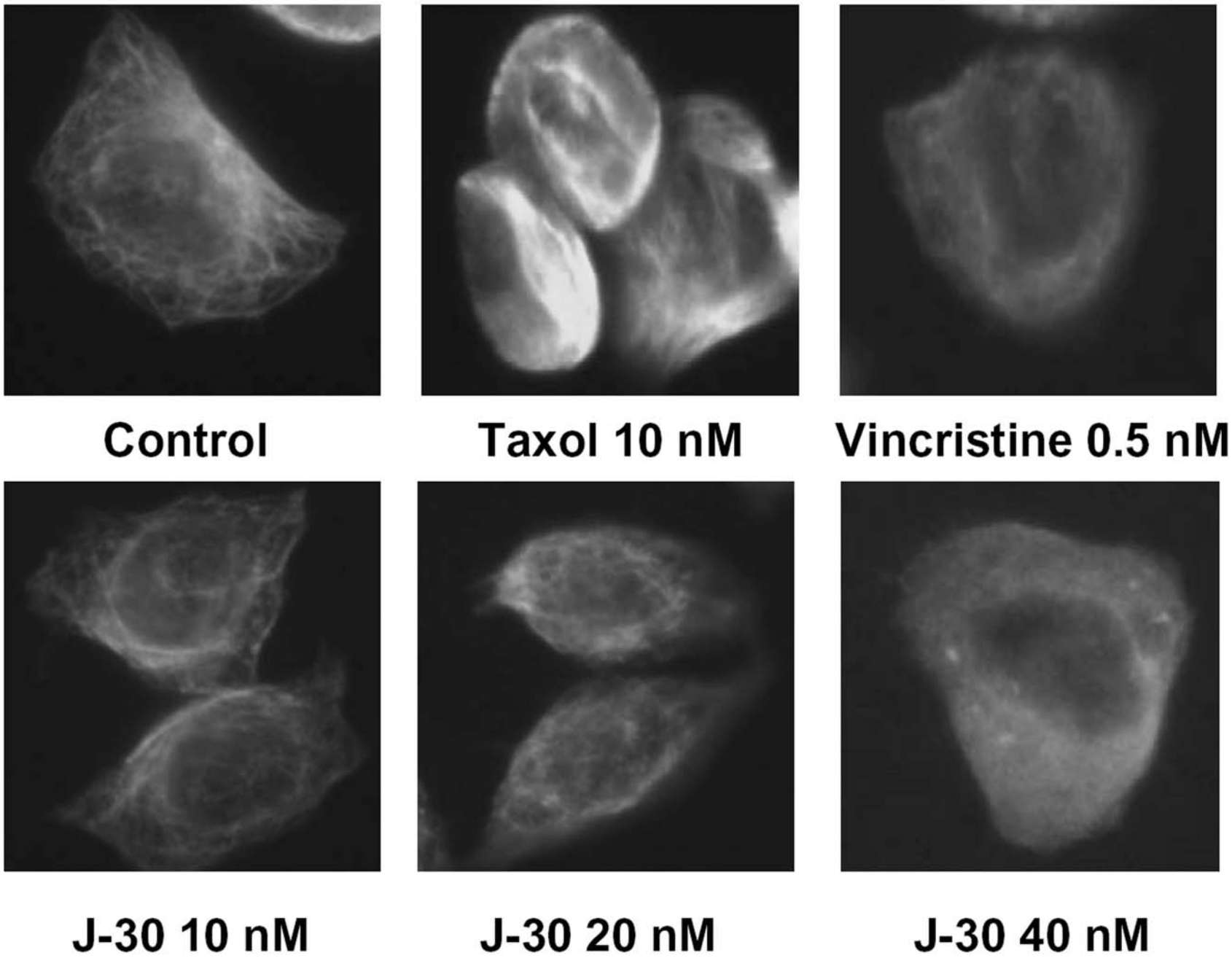

Figure 4A

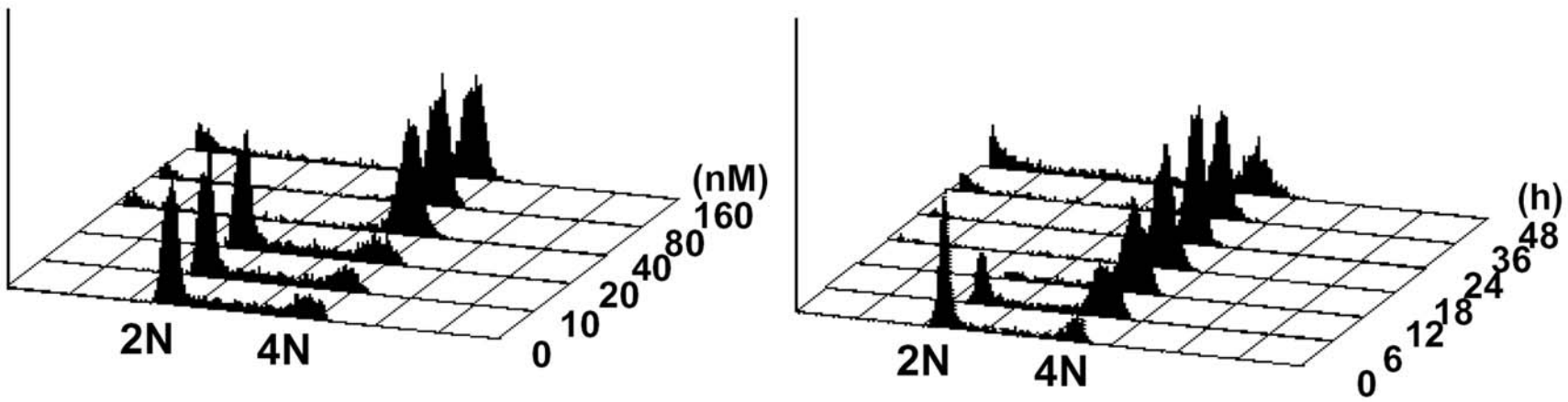

Figure 4B

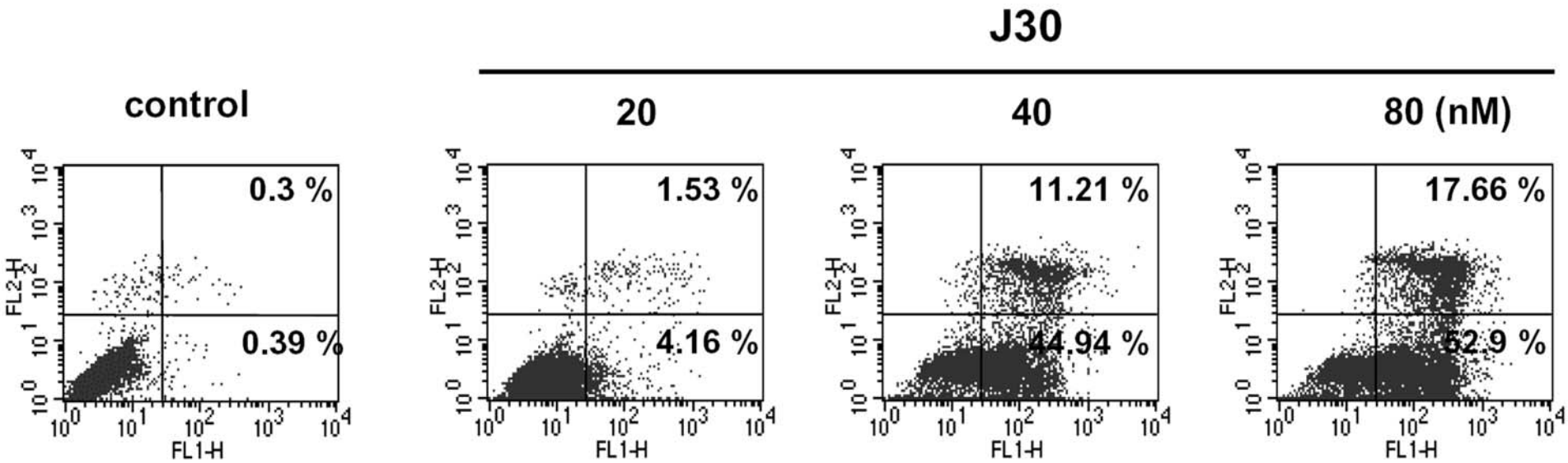

Figure 4C

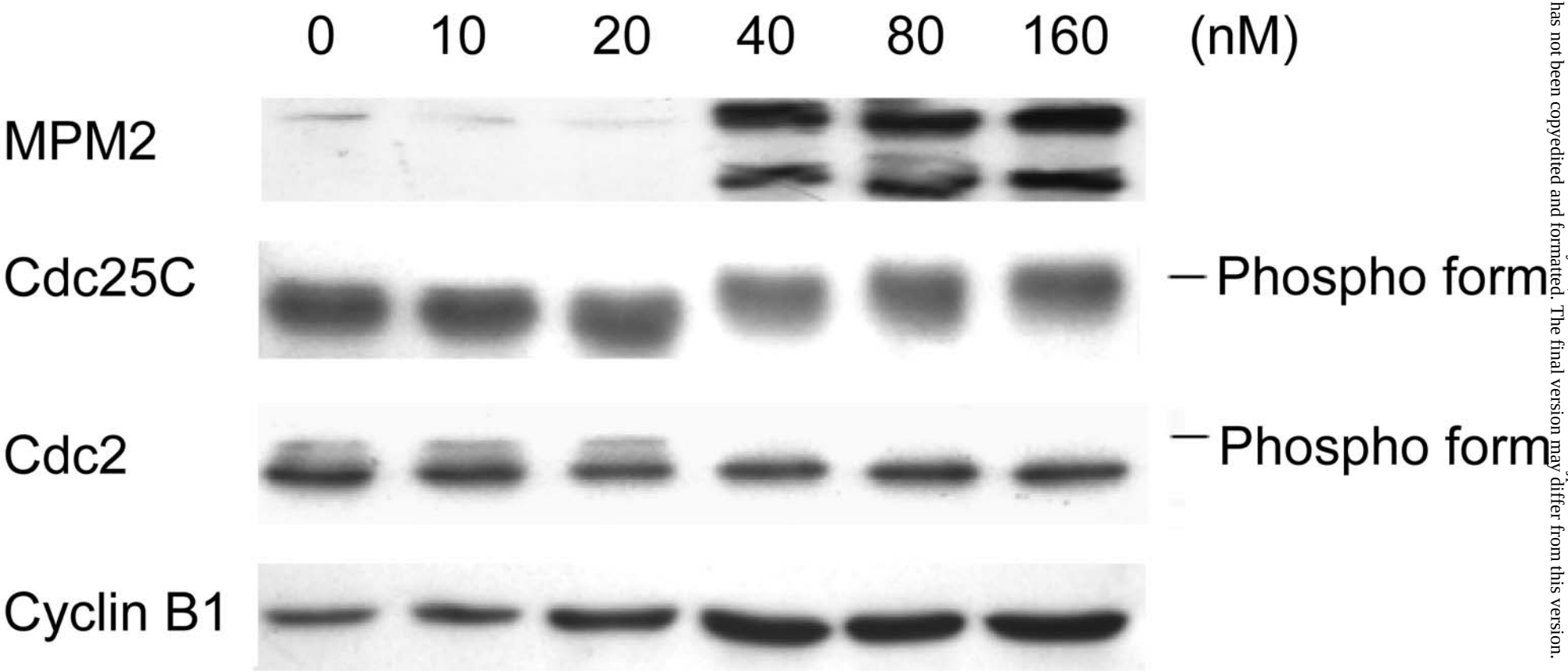

Figure 4D

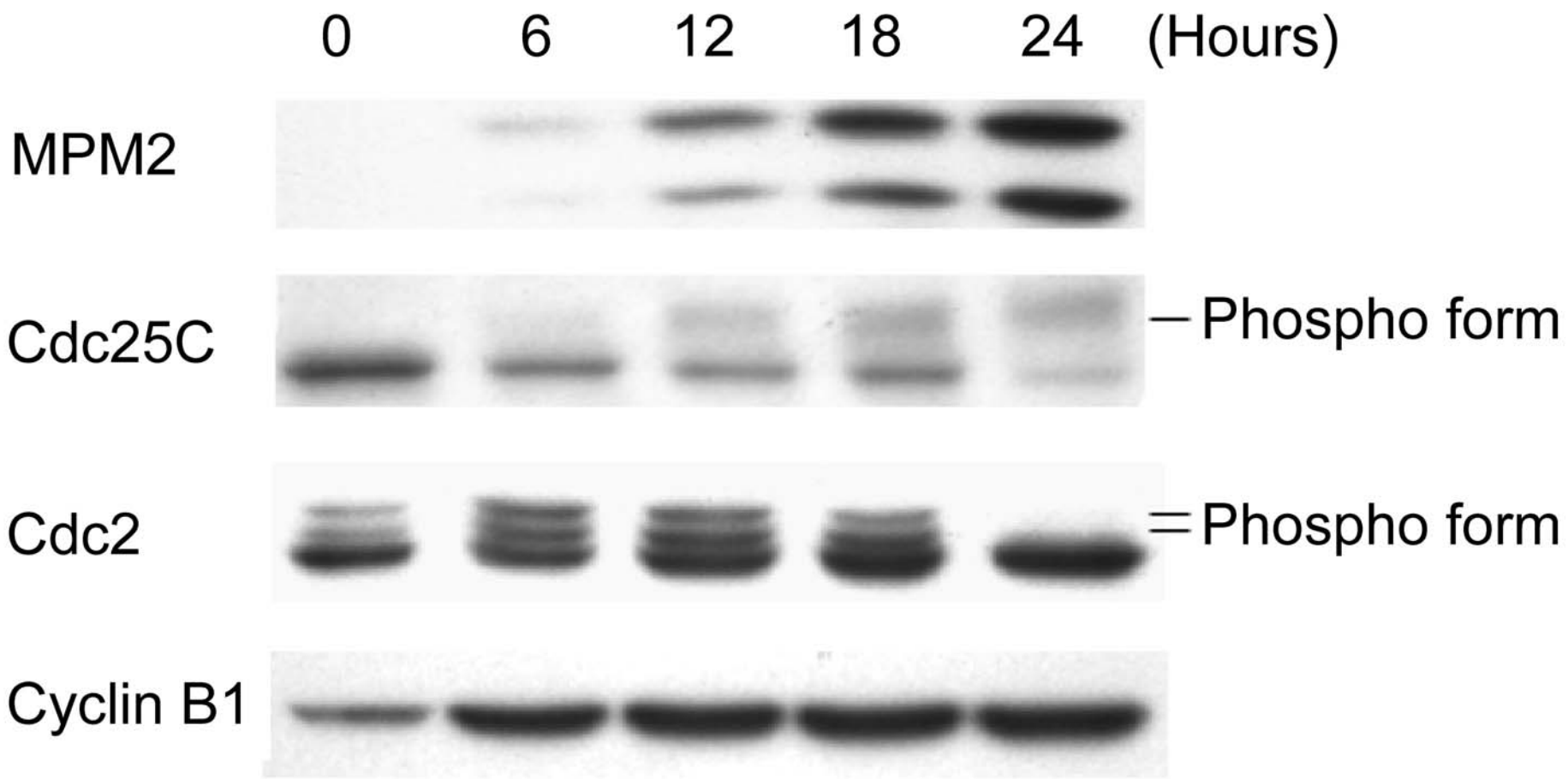

Figure 5A

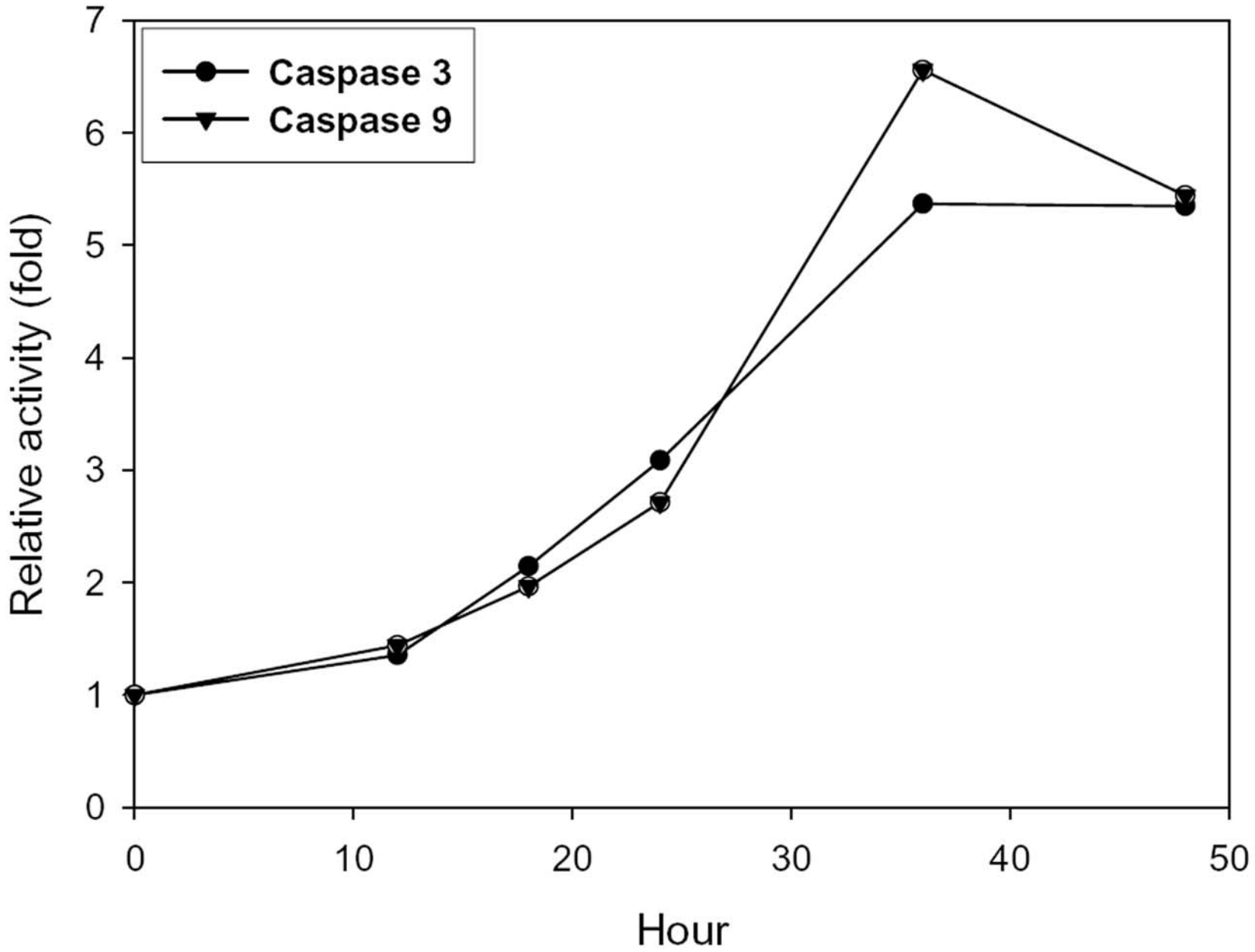

Figure 5B

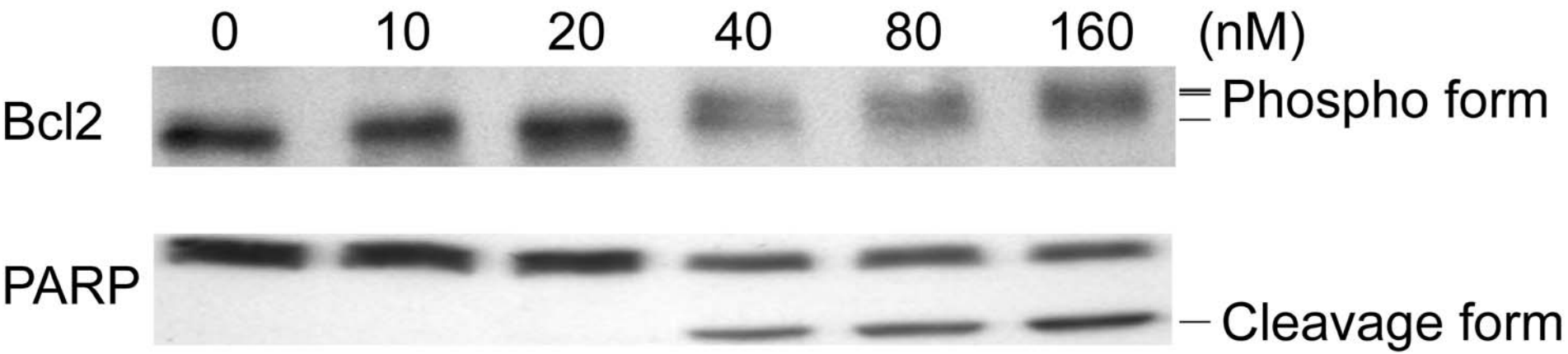

Figure 5C

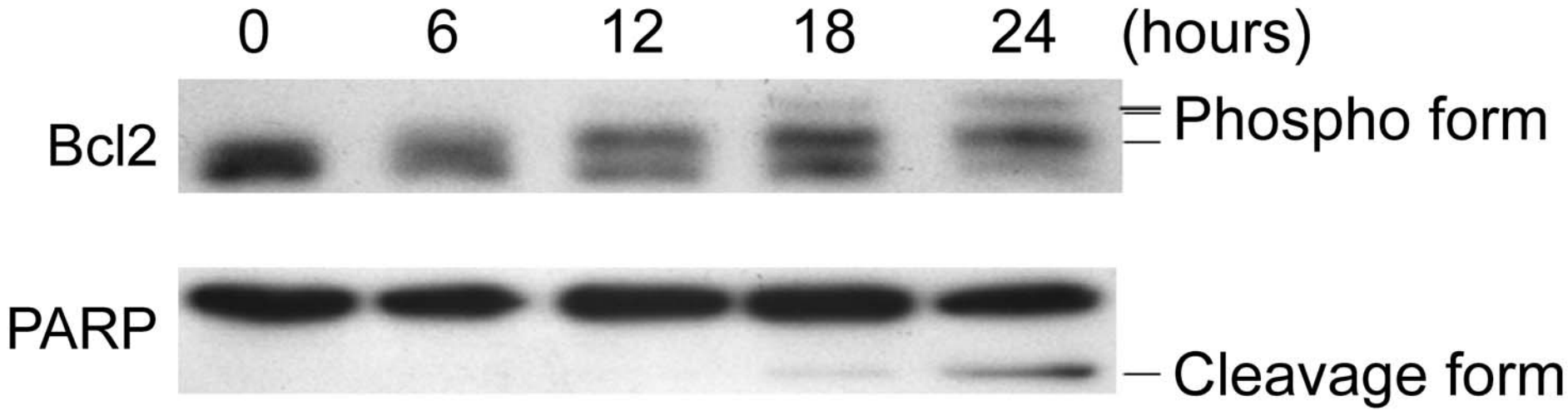

Figure 5D

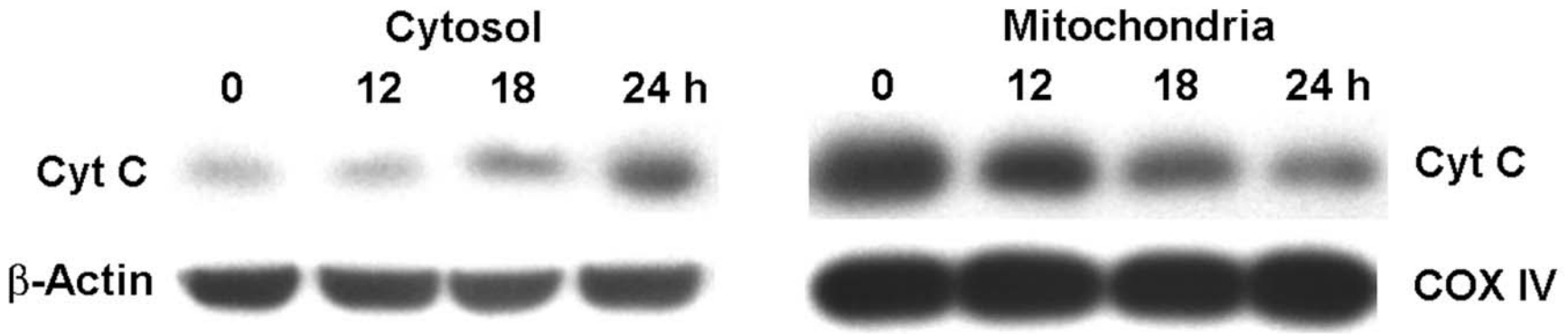

JPET Fast Forward. Published on July 27, 2007 as DOI: 10.1124/jpet.107.126680
This article has not been copyedited and formatted. The final version may differ from this version.

Figure 6A

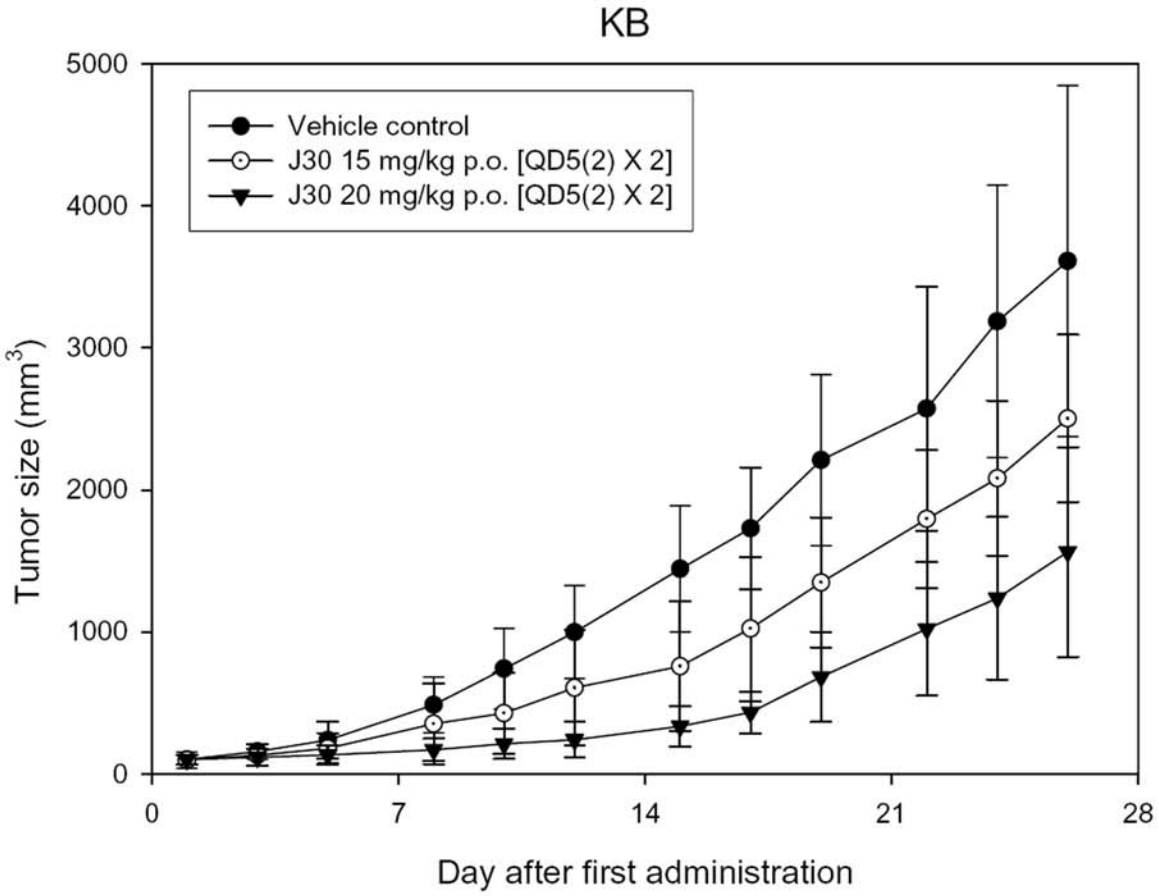

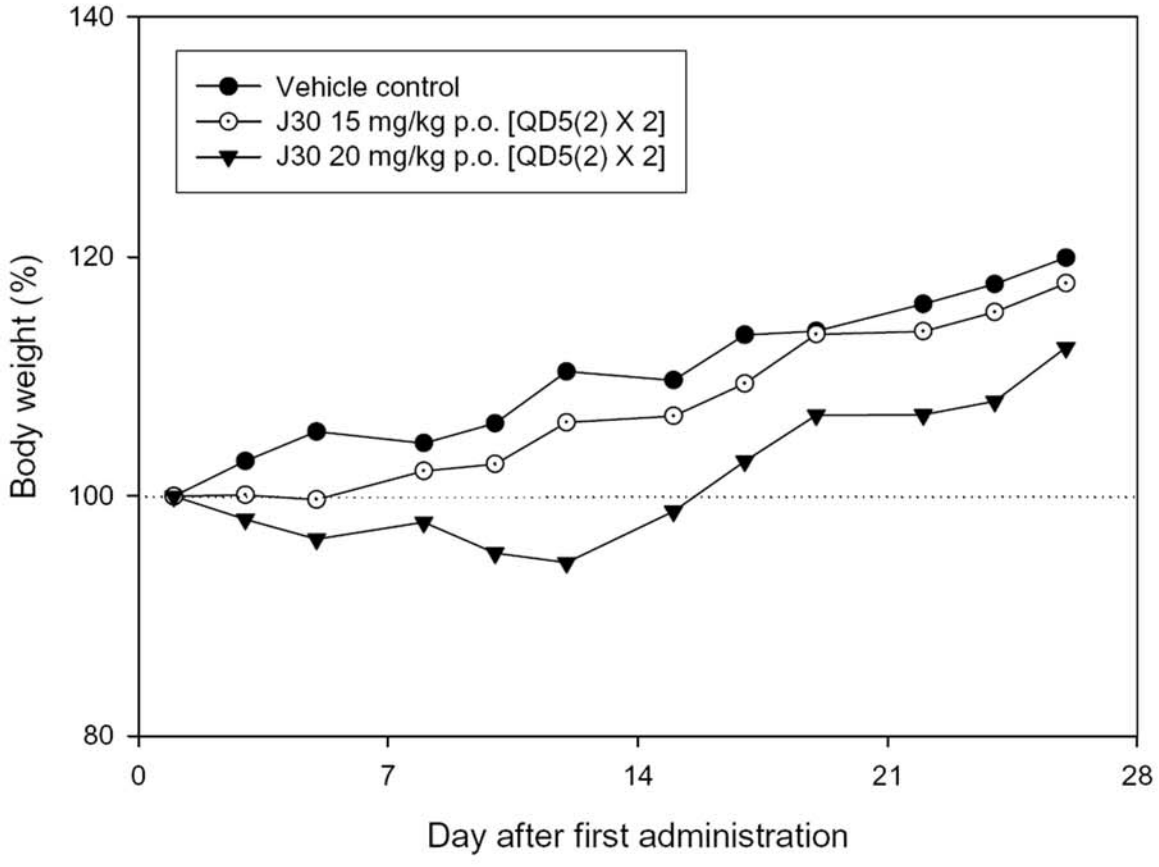

JPET Fast Forward. Published on July 27, 2007 as DOI: 10.1124/jpet.107.126680
This article has not been copyedited and formatted. The final version may differ from this version.

Figure 6B

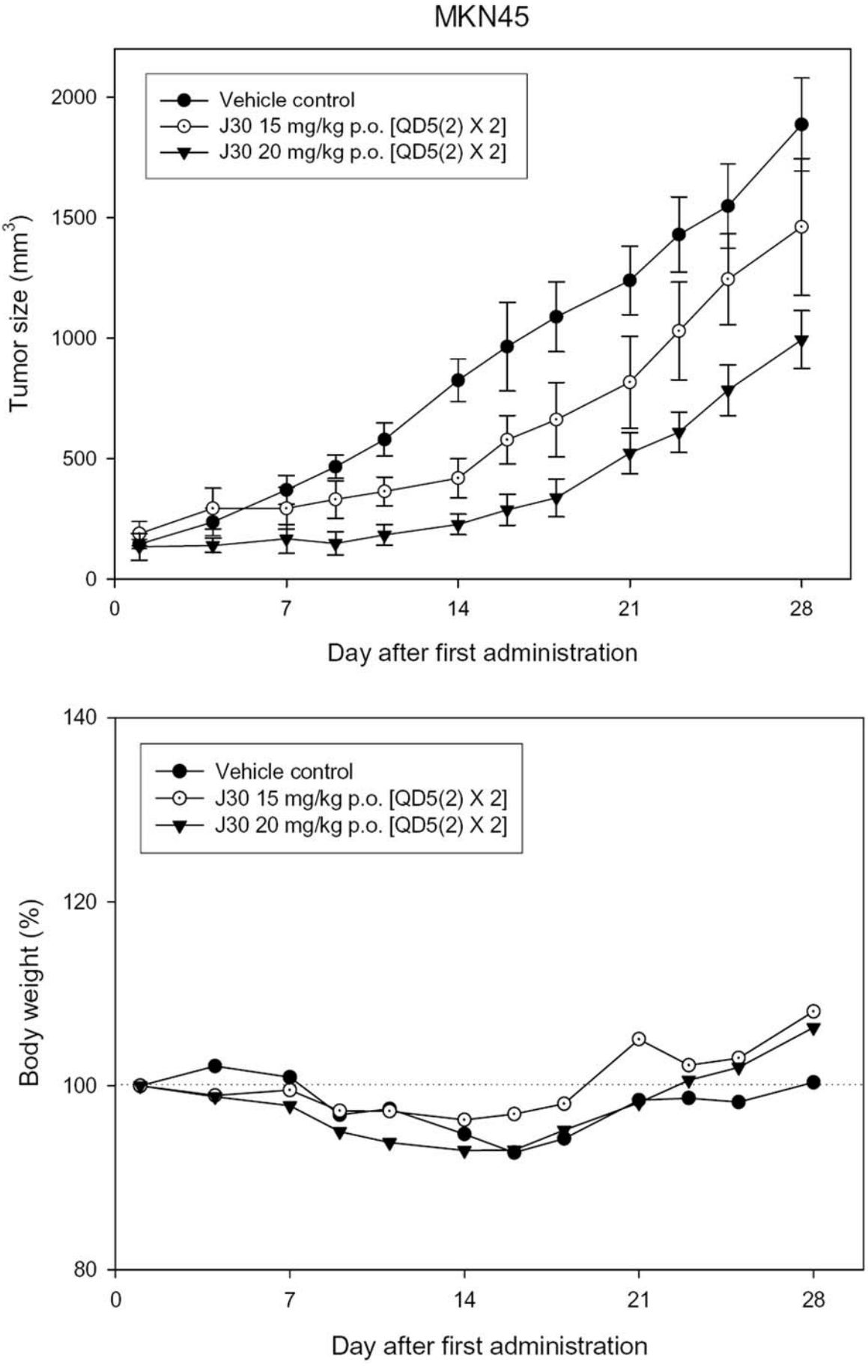

JPET Fast Forward. Published on July 27, 2007 as DOI: 10.1124/jpet.107.126680
This article has not been copyedited and formatted. The final version may differ from this version.

Figure 6C